International Research Journal of Engineering and Technology (IRJET) e-ISSN: 2395-0056
Volume: 08 Issue: 10 | Oct 2021 www.irjet.net p-ISSN: 2395-0072

Design and Computational Analysis of Continuous Groove Effect on the Wing

D T Venkatesh[1], Dr. N Chikkanna[2], Dr. Basawaraj[3], Sanjeev G Palekar[4], Anand M Raikar[5]

[1]*PG Student. Department of Aerospace Engineering, VTU CPGS, Muddenahalli, Chikkabalapura, Karnataka, India.*
[2]*Professor, Department of Aerospace Engineering, VTU CPGS, Muddenahalli, Chikkabalapura, Karnataka, India.*
[3]*Associate Professor, Department of Aerospace Engineering, VTU CPGS, Muddenahalli, Chikkabalapura, Karnataka, India.*
[4]*Assistant Professor, Department of Aerospace Engineering, VTU CPGS, Muddenahalli, Chikkabalapura, Karnataka, India.*
[5]*Design Engineer, Legend Technologies India. Pvt. Ltd, Doddanakundi, Bangalore, Karnataka, India*

Abstract - *Groove is a slight indentation on a surface. Groove create turbulence by creating vortices which delays the boundary layer separation resulting in decrease of drag, increasing aerodynamic efficiency, maneuverability and also the angle of stall. In the present work the flow characteristics of continuous groove on symmetric airfoil is investigated computational and compared with the smooth wing. Flow visualization is carried out in a Fluid condition at constant air flow at 15m/s with Reynolds no Re=1.019×10^5. The objective of this work is to determine how the Continuous grooves varies the flow characteristics of the wing section and to enhance the lift to drag ratio and reduce the boundary layer flow separation at various angle of attack and increase stall angle and study how the groove on the wing varies the flow characteristics. This can be achieved by wing section of NACA 0018 airfoil which is designed and analyzed for the further work. The design is done corresponding to calculated values which are taken as reference. The model is done in CATIA V5 software with desired specification. The analysis of the model is done using ANSYS WORKBENCH software applying subsonic flow. The aerodynamic forces i.e., lift and drag, are measured at 15m/s velocity at different angle of attacks.*

Key Words: Groove, Flow Visualization, **CATIA**-Computer-Aided Three-Dimensional Interactive Application, **AOA**-Angle of Attack

1. INTRODUCTION

Aircraft performance improvement can also be obtained through trailing edge optimization, control of the shock boundary layer interaction and of boundary layer separation. The drag coefficient of an object does not always remain the same as speed is changed. These changes in drag (coefficient) come about because the way the air behaves changes as speed and size are changed. Drag on an aircraft can be broadly classified into profile drag and induced drag. Additionally, drag due to the formation of shock wave also takes the role which is called as wave drag. By reducing the profile drag the total drag can be reduced. Improving the aerodynamic shape for commercial aircraft reduces the operating cost [1]. This improvement can be gained by concentrating on reducing the drag of an aircraft. Reducing the drag may lead to stall during landing. Hence stall angle should be improved by increasing the angle of attack. If the angle is increased the flow separation will also increase which will reduce the L/D ratio. Hence L/D ratio should be increased. This can be clearly studied using a low-speed aircraft.

A wing is a surface used to produce an aerodynamic force normal to the direction of motion by traveling in air or another gaseous medium, facilitating flight. It is a specific form of airfoil. The first use of the word was for the foremost limbs of birds but has been extended to include the wings of insects, bats and pterosaurs and also man-made devices. A wing is an extremely efficient device for generating lift. Its aerodynamic quality, expressed as a lift to drag ratio, can be up to 60 on some gliders and even more. This means that a significantly smaller thrust force can be applied to propel the wing through the air in order to obtain a specified lift. The most common use of wings is to fly by deflecting air downwards to produce lift, but upside-down wings are also commonly used as a way to produce down force and hold objects to the ground. The primary lifting surface of an aircraft is its wing. The wing has a finite length called its wing span. If the wing is sliced with a plane parallel to the XZ plane of the aircraft, the intersection of the wing surfaces with that plane is called an airfoil. This airfoil shape can different the slice is taken at different locations on the wing. However, for any given slice we have a given airfoil. We can now think of the airfoil as an infinitely long wing that has the same cross-sectional shape. Such a wing (airfoil) is called a two-dimensional (2D) wing. Therefore, when we refer to an

airfoil you can think of an infinite wing with the same cross-sectional shape. Since, calculating lift and drag coefficients with a reference area of infinity would not make sense, we take airfoil lift and drag coefficients for airfoils on the planform area assuming the span is unity.

Prasath M.S et.al, has studied the effects of dimples on aircraft wing. The experiment was carried out on airfoil NACA 0018 which has both inward and outward dimple placed 40% of chord from the leading edge. The surface having dimples successfully controls the flow separation and increases the lift force of an airfoil. Dimples delay the boundary layer separation by creating more turbulence over the surface thus reducing the wake formation. [Ref.1].

Deepanshu Srivastav et.al has studied to improve the maneuverability and performance of an aircraft by flow manipulation over the NACA 0018 airfoil. In his study dimples have increased the aerodynamic efficiency which therefore helps in improving the performance. [Ref.2].

M Moses Devaprasanna1 & N Maheswaran has done CFD study on aerodynamic effects of dimple on aircraft wings. Airfoil is a shape that enhances the aerodynamics and maneuverability of an aircraft. The wake region increases the pressure drag at higher angle of attack which is due to flow separation. Due to this effect the aircraft cannot elevate above an angle (i.e., stall angle). It is proposed to increase the stall angle by delaying the flow separation using dimples at various locations on the suction surface of the airfoil. [Ref.4]

Chowdhury H has studied on the effects of golf ball dimple configuration on aerodynamics, trajectory, that the flying distance of a golf ball is influenced not only by its material, but also by the aerodynamics of the dimple on its surface. The results showed that the lift coefficient of the golf ball increased if small dimples were added between the original dimples. [Ref.5]

The present study is to design and develop a model with continuous groove on the wing with actuations and enhance the lift to drag ratio, to delay the boundary layer flow separation and to increase the stall angle. Further analysis is carried for the different groove sizes and to determine the forces acting on it. After this, according to the required dimensions, the model is designed using CATIA V5. From CATIA software the model is imported to ANSYS and the forces acting on the wing are calculated and validated. Finally, the performance benefits offered by the continuous groove on the wing is compared and contrasted with that of the normal wing.

2. METHODOLOGY

Contributions in order to verify the proposed idea, an airfoil of NACA 0018 have been selected on which whole study will be based. This is a conceptual study which assumes an incompressible and isothermal flow. All the simulations are carried out on NACA 0018 airfoil, steady state analysis is considered here assuming turbulent flow. Reynolds number suggests the flow to be fully turbulent. The calculated values of NACA 0018 airfoil are taken as a reference for our project. By using these values, the model with continuous groove wing is designed in CATIA software. Later the model from the CATIA software is imported into the ANSYS software. The model is analyzed with various flow properties like pressure contour, velocity contour. The model is set to different degrees and conclusion is drawn to conclude which type of design configuration will give maximum lift and better flow properties.

3. MODELLING

The Dimension of the NACA 0018 Airfoil is taken from referring many researches works as shown in Fig 1. The coordinates are imported in CATIA USING Excel sheet and a 2D model is generated by connecting airfoil Coordinates.

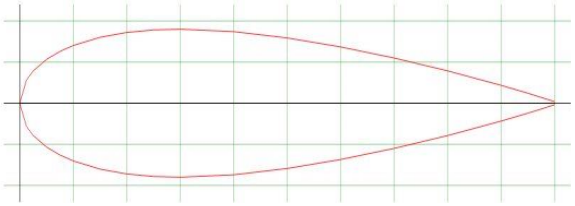

Fig 1: Airfoil Dimensions

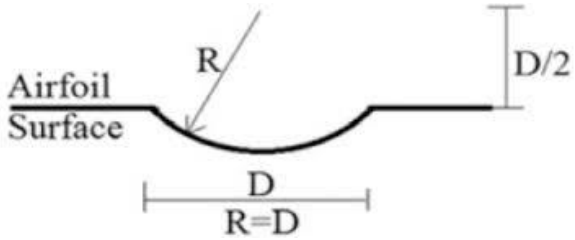

Fig 2: 2D view of groove sizing

The groove over the airfoil is done using the above figure shown in Fig 2.

3.1 3D Modelling

3D modelling is done using CATIA V5 software, coordinates obtained from the website www.airfoiltools.com are imported to CATIA V5. Models has been prepared to compare the lift generated with different models.

The models are:

- Wing without groove.
- Wing with 7mm groove at 25% of chord.
- Wing with 7mm groove at 50% of chord.
- Wing with 3mm groove at 10% of chord.

The designed models are shown below:

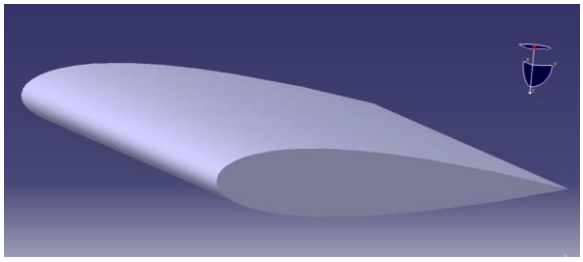

Fig 3: Wing without groove.

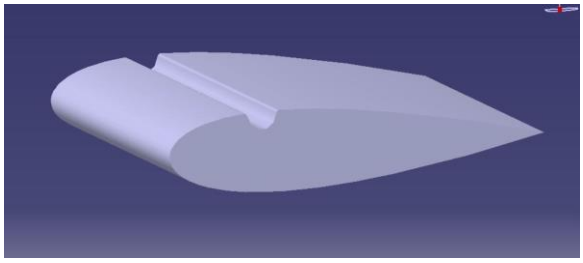

Fig 4: Wing with 7mm groove at 25% of chord.

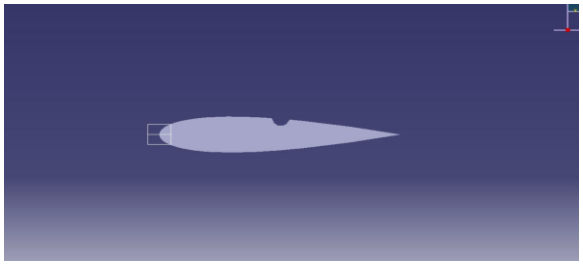

Fig 5: Wing with 7mm groove at 50% of chord.

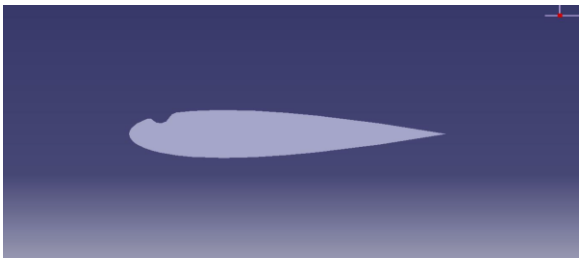

Fig 6: Wing with 3mm groove at 10% of chord.

4. MESHING

An environment consisting of rectangle surrounds the NACA 0018 airfoil. The mesh is constructed to be very fine at regions close to the airfoil and with high energy and coarser farther away from the airfoil. For this airfoil a structured quadratic mesh was used.

Due to limitations in the FLUENT software, the mesh has to be fine also in certain regions far from the airfoil. For the NACA 0018 airfoil, the very front has an edge grid distributed with an increasing distance between nodes starting from very small sizes.

Different sizing for mesh is selected by selecting course, medium and fine in fluent meshing.

- Importing the model into ANSYS FLUENT MESH.
- Naming the different sections of the test section.
- Meshing is done for different meshing size.

Then we generate the mesh for further solution.

4.1 Boundary Conditions

INLET

The inlet velocity (u) is 15 m/sec for a free stream Reynolds number of 1×105 and air at STP (Temperature=300K, Pressure=1.01325 bar) as the fluid medium.

Turbulent intensity and viscosity ratio conditions are set to a value of 5 as per the industry practices.

OUTLET

Ambient atmospheric condition is imposed at outlet.

WALL

No slip boundary conditions are imposed. The airfoil surface is treated as wall boundary.

Assumptions

The flow is steady, one dimensional, viscid, incompressible and turbulent.

Table 1: ANSYS analysis parameters

Parameters	Description
Solver	Double Precision
Solver Type	Pressure Based
Velocity Formulation	Absolute and steady
Reference density	1.225 kg/m3
Dynamic Viscosity	1.7894x10-5 kg/m-s.
Viscous Model	STD k- ω, standard wall function.

4.2 Grid Independency Test for Plain Wing At 10° AOA

The table 2 Shows the Grid independency study on plain wing at 10° AOA and the CL, CD, Lift to drag ratio obtained from the results is mentioned

Table 2: Grid independency test for plain wing at 10° AOA

Min Face Size	Max Face Size	Max Tet Size	Growth Rate	Element	Aspect Ratio	CL	CD	CL/CD
0.07	2	5	1.20	1682778	45.0	0.352	0.0322	10.90
0.05	1.6	5	1.20	2647581	50.1	0.350	0.0318	10.99
0.04	1.4	5	1.20	3450844	49.7	0.348	0.0314	11.07
0.04	1.3	5	1.20	3587212	43.3	0.344	0.0310	11.09

4.3 VALUES OF PLAIN WING AND GROOVE WING MODEL WITH AOA

Table 3: Values for plain wing with different AOA

AOA	CL	CD	CL/CD
5	0.1818	0.0267	6.796
10	0.3522	0.0323	10.89
12	0.4197	0.0432	9.907
14	0.4309	0.0781	7.416
15	0.4284	0.2164	6.447
16	0.3528	0.0738	4.789
18	0.3461	0.1381	2.495

Table 4: Values of 7mm groove at 50% of chord with AOA

Minimum Face Size	Maximum Face Size	Maximum Tet Size	Growth Rate	Element	AR	CL	CD	CL/CD	AOA
0.07	2	5	1.20	2233146	75.8	0.144	0.0253	5.72	5
0.07	2	5	1.20	2243671	82.3	0.355	0.0393	9.02	10
0.07	2	5	1.20	2204538	154	0.395	0.0483	8.26	12
0.07	2	5	1.20	2215637	116	0.445	0.0621	7.16	14
0.07	2	5	1.20	2209943	117	0.463	0.0637	7.26	15
0.07	2	5	1.20	2231893	118	0.503	0.3102	16.1	16
0.07	2	5	1.20	2242796	124	0.379	0.1345	2.83	18

Table 5: Values of 7mm groove at 25% of chord with AOA

Minimum Face Size	Maximum Face Size	Maximum Tet Size	Growth Rate	Element	AR	CL	CD	CL/CD	AOA
0.07	2	5	1.20	2196542	11.8	0.1448	0.0233	6.11	5
0.07	2	5	1.20	2233976	57.1	0.3551	0.0393	9.02	10
0.07	2	5	1.20	2219489	117	0.3656	0.0719	5.08	14
0.07	2	5	1.20	2269841	230	0.3591	0.0862	4.16	15

Table 6: Values of 3mm groove at 10% of chord with AOA

Minimum Face Size	Maximum Face Size	Maximum Tet Size	Growth Rate	Element	AR	CL	CD	CL/CD	AOA
0.07	2	5	1.20	1824850	55.4	0.355	0.058	6.02	12
0.07	2	5	1.20	1876543	572	0.399	0.049	8.03	14
0.07	2	5	1.20	1902039	584	0.442	0.041	10.77	15
0.07	2	5	1.20	1978646	589	0.423	0.069	7.13	16

14	0.4289	0.0632
15	0.4771	0.0652
16	0.4926	0.3502
18	0.3649	0.1129

5. RESULTS AND DISCUSSION

5.1 Simulation Comparative Study

Validation process was carried out in order to compare results that were obtained through simulation, for wing model 7mm groove placed at 50% of the chord, 7mm groove placed at 25% of the chord and 3mm groove placed at 10% of the chord for different angle of attack.

The simulation findings in the table demonstrate that, compared to other wings, the wing with 7mm groove is positioned at 50 % of the chord at 16° AOA CL / CD and may generate higher lift.

5.2 Results of Simulation

The table 7 displays test results for lifting and drags coefficients from 0° to 18° for the angle of attack.

Table-7: Test results for NACA 0018 7mm groove at 50% chord Re=1.09x105

Angle of attack (°)	Lift Co-efficient (CL)	Drag Co-efficient (CD)
5	0.1335	0.0282
10	0.3398	0.0381
12	0.3798	0.0488

Above Table 7 displays the test results for NACA 0018 airfoil at Reynolds number of 1.09x105, equivalent to velocity 15 m/s, which is in the incompressible flow domain. At stalling attack, the highest lift coefficient is 0.4926 and the drag coefficient corresponds to 0.3502.

Table 8 provide the lifting and drag coefficients of 0° to 18° from the basic k-omega model. The results are compared with the test results from experiments or wind tunnels.

Table 8: Results of CFD study for the 50 percent chord Re=1,09x105 NACAs for 0018 7 mm groove, calculated of viscous k-omega standard model

AOA (°)	Lift and drag forces computed by viscous STD k-omega	
	Lift Co-efficient (CL)	Drag co-efficient (CD)
5	0.1448	0.02536
10	0.3551	0.03935
12	0.3995	0.04834
14	0.4453	0.06214
15	0.4631	0.06376
16	0.5023	0.31021
18	0.3798	0.13456

The below graphs Fig 7 and Fig 8 are the comparison of Lift Coefficient (CL) and Drag Coefficient (CD) with respect to Angle of attack (AOA). The results which are obtained from the computational Analysis are validated with the results which are obtained from the similar analysis report [2].

As you can see the graphs the results which are obtained by our results shows that we have achieved more Lift and Less Drag Coefficient.

Now we compare our different types of wing with and without Grooves for the further comparison to obtain the best model design to achieve less drag and more lift coefficient and get the brief knowledge about the Flow separation and Vortex flow over the wing.

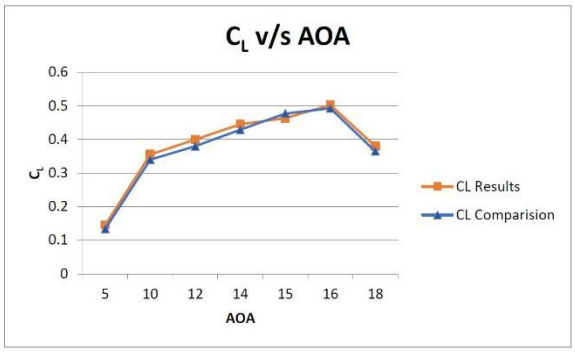

Fig 7: CL v/s AOA of Analysis Results and Comparison Results

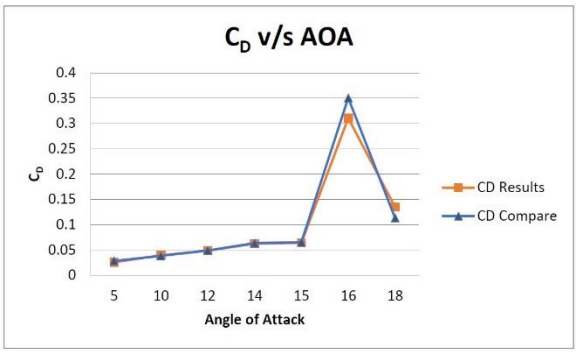

Fig 8: CD v/s AOA of analysis Results and Comparison Results

5.3 Plain Wing

5.3.1 Pressure Contour, Velocity Contour and velocity vector at different AOA

The Figure 9 Shows the Pressure contour, Velocity Contour and Velocity Vector respectively. Where in the pressure contour the upper surface of the wing has low pressure and the lower surface has high pressure as the lower surface is facing the flow of air at 15m/s at 10° AOA. This demonstrates that the lower side pressure tries to raise the body and hence increase the lift factor. In the velocity Contour you can observe reddish color that at top surface explains high velocity air flow over the wing and the velocity vector shows the flow of air over the plain wing which shows about 75% of chord the flow separation starts near the trailing Edge when the wing is placed at 10° AOA.

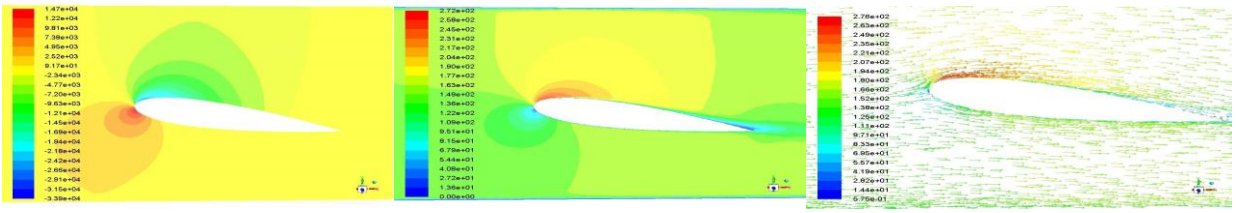

Fig. 9: Static pressure contour, Static velocity contour, Velocity vector at 10° AOA

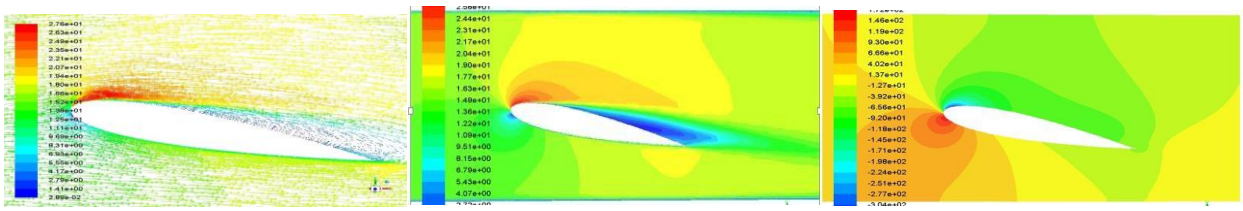

Fig. 10: Velocity vector, Static velocity contour, Static pressure contour at 16° AOA

The Figure 10 Shows the Velocity Vector, Velocity Contour and Pressure contour respectively. The velocity vector shows that the reddish color over the top surface illustrates the high air velocity flow and blue color represents the less air flow We notice that there is a significant gap between the vector at the trailing edge that suggests that the flow is already divided, which leads to stagnation. The top surface with a low pressure and the lower surface with a high pressure are evident from the below velocity contours. Where in the pressure contour the upper surface of the wing has low pressure and the lower surface has high pressure as the lower surface is facing the flow of air at 15m/s at 16° AOA. This demonstrates that the lower side pressure tries to raise the body and hence lift is obtained. However, the flow separation at the leading edge causes a stall angle over 16° angle of attack lift.

The Figure 11 shows Static pressure contour, Velocity vector, Static velocity contour respectively at 18° AOA. In this the lift angle of attack begins to decrease for the plain wing due to the flow-separation at the top of the wing, which causes the stable angles, the full flux-unit at 18° is shown to increase the pressure at the top of the wing model. From the velocity vector Fig, you can clearly observe that there is no lift generated at 18° causing the failure of wing body and occur stall.

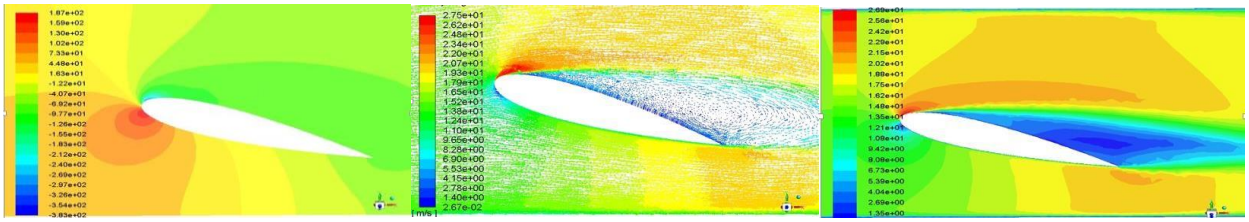

Fig. 11: Static pressure contour, Velocity vector, Static velocity contour at 18° AOA

5.4 7mm Groove at 50% of Chord

5.4.1 Pressure Contour, Velocity Contour and velocity vector at different AOA

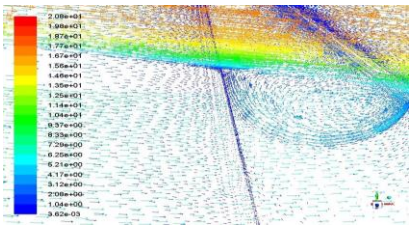

Fig 12: Velocity vector near 7mm groove at 50% chord

In the velocity contour from the figure 12 you can see that there is vortex formation at 50% of chord which clearly indicates that the groove delays the flow separation causing the increase in lift coefficient.

In the figure 13 you can Observe that there is a groove place at 50% of Chord as the AOA is 5° there is no such effect of grove is observed. The pressure on the leading edge is 131Pa and the pressure on the trailing edge is 18Pa, such that the static pressure on the top surface is lower than the lower surface.

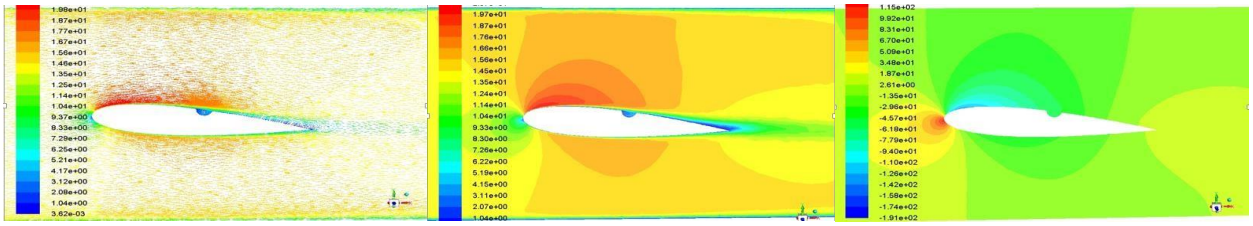

Fig. 13: Velocity vector, Static velocity contour, Static pressure contour at 5° AOA

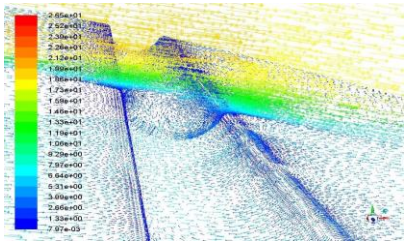

Fig 14: Velocity vector at 10° AOA

The velocity vector for the 7mm grove at 50 % chord is shown in fig 14 Here the wing is tilted upward by 10° AOA Here the vortex formation or the recirculation of the air foil can be observed from the fig. As we know flow separation increases as the attack angle increases, but the positioning of the groove causes a turbulence because of the flow reconnection taking place.

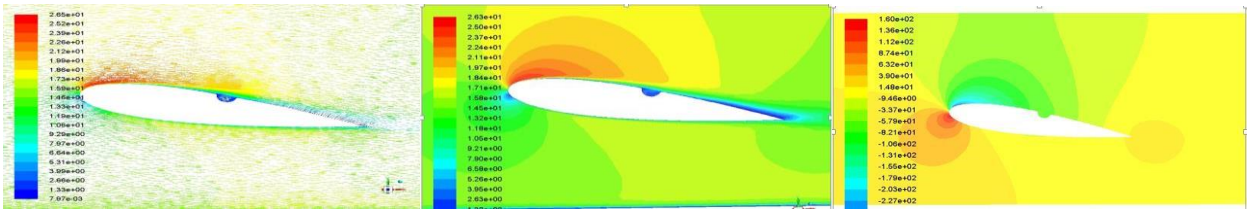

Fig. 15: Velocity vector, Static velocity contour, Static pressure contour at 10° AOA

The Velocity Contour of the 7mm groove at 50 % chord in the mid-section of the span is illustrated in Fig 15. In this figure there is a high speed on the top surface of the lower surface for the velocity contour. The velocity is 26.3m/s at the leading speed and almost nil at the trailing edge.

The static pressure Contour for the 7mm groove at 50% C on the mid-range portion is illustrated in Figure 15. The red color is a higher-pressure value of 160 Pa and greenish indicates a lower pressure value of -57.9Pa. since the increase in AOA the lifting factor Increases.

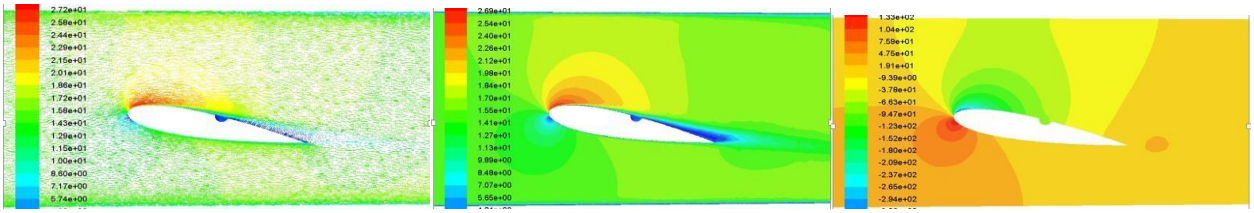

Fig. 16: Velocity vector, Static velocity contour, Static pressure contour at 12° AOA

Fig. 17: Velocity vector Static velocity contour Static pressure contour at 14° AOA

Fig. 18: Velocity vector, Static velocity contour, Static pressure contour at 15° AOA

The Fig 15, Fig 16, Fig 17 Shows the velocity vector, velocity Contour and pressure contour for 12°, 14°, 15° AOA respectively. These figures clearly show the delay in flow separation in various AOA resulting in obtaining more Lift Co-efficient than normal Plain Wing.

The Fig 19 it shows the velocity vector and it is seen that the flow separation is comparatively less when compared to normal wing at the same angle of attack, due to placement of groove the turbulence caused by it reattaches the flow thus increasing lift and the stall angle. The Fig 19 shows the contours of velocity and pressure for 7mm groove placed at 50% of chord. Here, we can see that there is high pressure acting on the lower surface when compared to other model this means lift is high at this angle of attack and in velocity contour shows high velocity is at leading edge due to angle of attack.

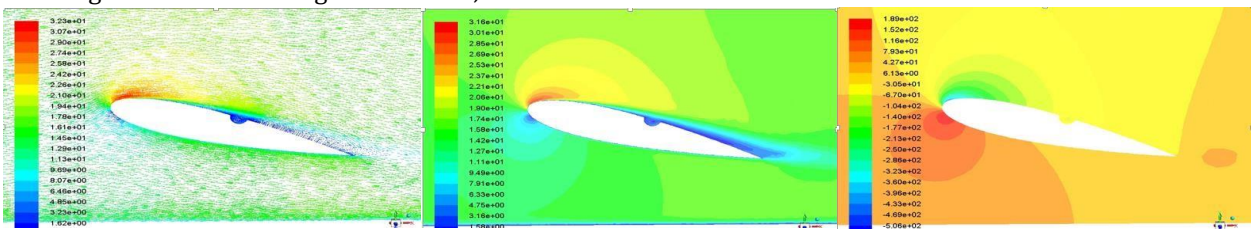

Fig. 19: Velocity vector, Static velocity contour, Static pressure contour at 16° AOA

The Fig 20 shows the velocity vector, it clearly shows that there is boundary layer flow separation as angle of attack increases causing stall angle, hence above this angle of attack lift will gradually decrease.

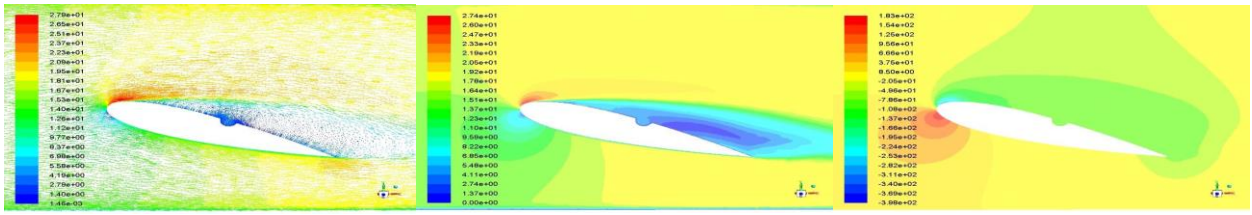

Fig. 20: Velocity vector, Static velocity contour, Static pressure contour at 18° AOA

The Fig 20 shows the contours of velocity and pressure for 7mm groove placed at 50% of chord. Here, we can see that the pressure acting on the lower surface is lesser when compared to groove model at 16° angle of attack, this means lift is comparatively less at this angle of attack and in the velocity, contour shows high velocity is at leading edge of upper surface due to angle of attack.

5.5 7mm GROOVE AT 25% OF CHORD

5.5.1 Pressure Contour, Velocity Contour and velocity vector at different AOA

The Fig 21 shows the contours of velocity and pressure for 7mm groove placed at 25% of chord. Here, we can see that the velocity acting on the upper surface is reddish color which means high velocity and at trailing edge it is bluish color means low velocity. The groove placed at 25% of chord is not playing any vital role when compared to groove placed 50% of chord at same angle of attack to attain better lift. Pressure contour shows the pressure distribution on the both surfaces, we can see that there is high pressure at the leading edge which is red in color.

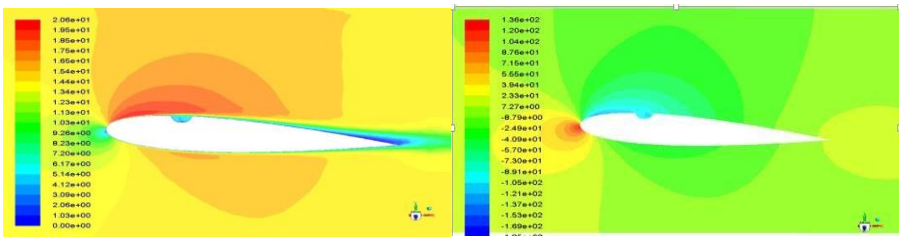

Fig. 21: Static velocity contour, Static pressure contour at 5° AOA

The Fig 22 shows velocity vector and pressure contour, the velocity vector at 10° angle of attack at the mid-section span is shown, and it is seen that there is a recirculation due to placement of groove at 25% of chord. It is seen that groove placed at the 25% of chord is not giving better lift when compared to model having groove 50% of chord. And from the pressure contour we see that at leading edge there is high pressure acting at the lower surface.

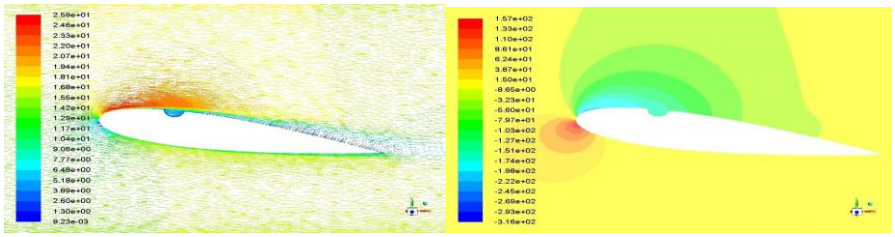

Fig. 22: Velocity vector, Static pressure contour at 10° AOA

From the below Fig 23, the velocity vector at 14° angle of attack at the mid-section span is shown, and it is seen that there is a recirculation due to placement of groove at 25% of chord. It is seen that groove placed at the 25% of chord is not giving better lift when compared to model having groove 50% of chord.

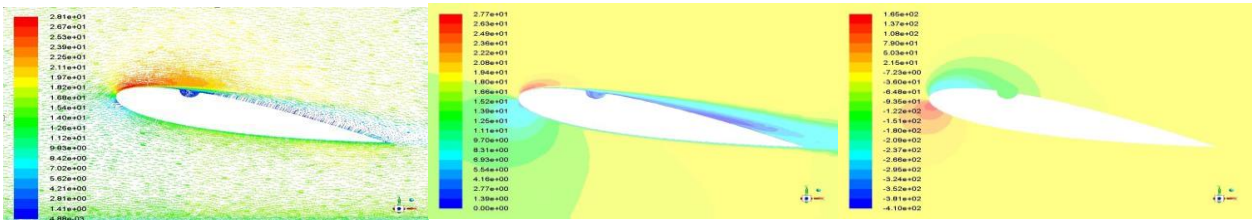

Fig. 23: Velocity vector, Static velocity contour, Static pressure contour at 14° AOA

From the Fig 23, it shows contours of static pressure and velocity of 7mm groove placed at 25% of chord at mid-section span length. It is seen that the flow separation is occurring and the turbulence caused by the groove is this angle of attack is not comparatively efficient than the groove placed at 50% of chord for the same angle of attack. Here we can also see that the pressure at the leading edge of lower surface more that is 165 Pa and the maximum velocity at the upper surface of leading edge.

5.6 3mm GROOVE AT 10% OF CHORD

5.6.1 Pressure Contour, Velocity Contour and velocity vector at different AOA

The Fig 24 shows the velocity vector for 3mm groove placed at 10% of chord. Here we can see that the turbulence caused by the groove is trying to reattach the boundary layer but it not comparatively better when compared to 7mm groove at 50% of chord and comparatively better than plain wing at same angle of attack.

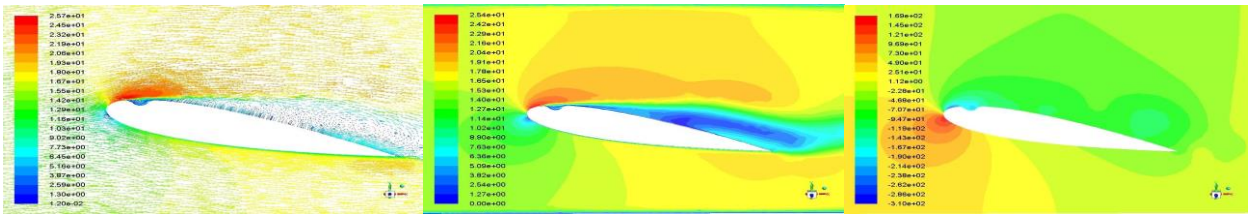

Fig. 24: Velocity vector, Static velocity contour, Static pressure contour at 14° AOA

The Fig 24 shows the pressure and velocity contours, as it is clearly seen that the flow is reattaching near the groove downstream but later it increases more, this model also gives the good result when compared to plain wing at 10° AOA at 15 m/s.

In the below Fig 25 shows the velocity vector of 3mm groove placed at 10% of chord at 14.5° angle of attack. It is seen that from velocity vector there is flow separation at upper surface, there is a recirculation due to placement of the groove where the flow tries to recirculate near it causing to reattachment of flow, for some distance flow is reattached and later it increases as shown below.

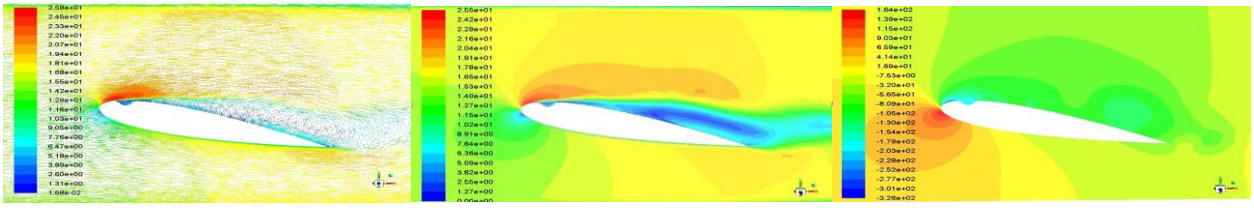

Fig. 25: Velocity vector, Static velocity contour, Static pressure contour at 14.5° AOA

In the Fig 25, the static contours of velocity and pressure are shown which shows the pressure distribution of flow on the both surfaces, at leading edge there is high pressure acting and velocity is high at the upper surface. Lift produced by model is comparatively more when compared to plain wing and less when compared to wing having 7mm groove at 50% of chord.

The Fig 26 shows the velocity vector of 3mm groove placed at 10% of chord at 15° angle of attack. It is seen that from velocity vector there is flow separation at upper surface, there is a recirculation due to placement of the groove where the flow tries to recirculate near it causing to reattachment of flow, for some distance flow is reattached and later it increases as shown below.

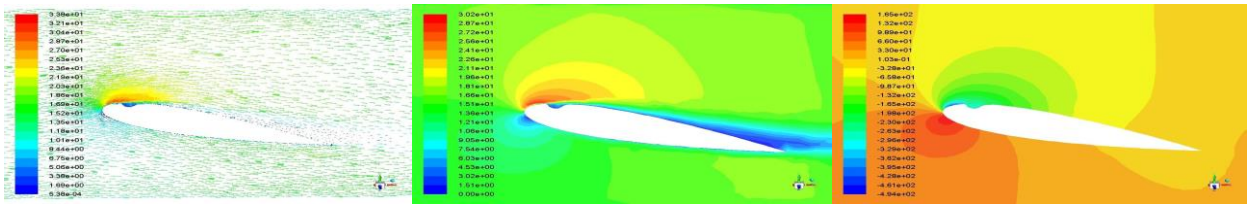

Fig. 26: Velocity vector, Static velocity contour, Static pressure contour at 15 ° AOA

The static velocity and pressure contours are illustrated in Fig 26, showing a pressure distribution of the flow on both surfaces, at leading edge of lower surface there is high pressure acting and velocity is high at the upper surface. Lift produced by model is comparatively more when compared to plain wing and less when compared to wing having 7mm groove at 50% of chord and the stall angle of this model is increased with this groove.

The Fig 27 shows the velocity vector of 3mm groove placed at 10% of chord at 16° angle of attack. It is seen that from velocity vector there is flow separation at upper surface there is a recirculation due to placement of the groove where the flow tries to recirculate, but due to high angle of attack the flow separation takes place.

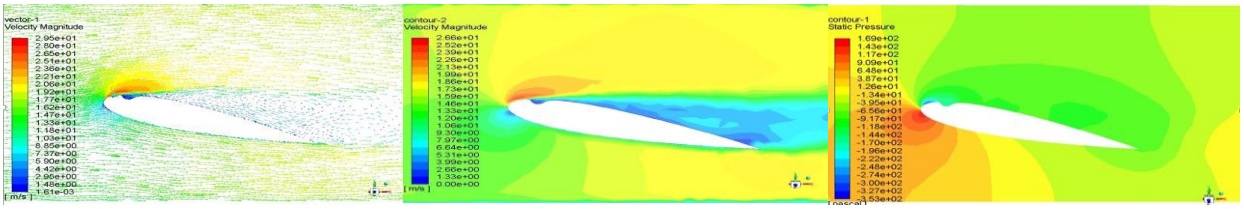

Fig. 27: Velocity vector, Static velocity contour, Static pressure contour at 16° AOA

In the Fig 27 the static contours of velocity and pressure are shown which shows the pressure distribution of flow on the both surfaces, at leading edge of lower surface there is high pressure acting and velocity is high at the upper surface. At this angle of attack the lift reduces causing the flow separation.

5.7 Calculation of Reynolds Number and Mach Number

$$R_e = \frac{\rho \times V \times C}{\mu}$$

$$R_e = \frac{1.22 \times 15 \times 0.101}{1.7 \times 10^5}$$

$$R_e = 1.019 \times 10^5$$

$$M = \frac{V}{a}$$

$$M = \frac{15}{334} = 0.045$$

5.8 Verification with Prandtl Lifting Line Theory

Here we will get the value of CL for 2D airfoil from the airfoil plotter. Then we will check the value of CL for our 3D airfoil by applying Prandtl formulae for 2D and 3D airfoil.

$$C_L = a_0 \times \propto \quad \text{For 2D airfoil}$$

$$\mathbf{1.1232 = a_0 \times 0.2443}$$

$$\boldsymbol{a_0 = 4.59}$$

From the website for 2D airfoil we got CL as 1.1232 at 14 degree and we have to check for our 3D airfoil by substituting the values in the above formula. If we get the value of CL ranging from 0.4 to 0.5 then our analysis and experimental values are correct.

$$C_L = a \times \propto \text{ For 3D Airfoil}$$

$$C_L = 1.707 \times 0.2443$$

$$C_L = 0.417$$

5.9 Aerodynamic Force Calculations

The Lift is calculated as

$$L = q_\infty \times S \times C_L$$

The Drag is calculated as

$$D = q_\infty \times S \times C_D$$

$$q_\infty = \frac{1}{2}\rho V^2$$

$$q_\infty = \frac{1}{2} \times 1.225 \times 152$$

$$q_\infty = 137.81 \text{ N/m2}$$

S = 0.02525 m2

L = 137.81 x 0.02525 x 0.5023

L = 1.747 N

D = 137.81 x 0.02525 x 0.031

D = 0.1078 N

The lift and drag are calculated for the wing with groove 7mm at 50% of chord with different angle of attacks.

5.10 COMPARATIVE STUDY

The comparison between the normal wing and 7mm groove wing at 25% chord is shown below in Fig 30 and Fig 31. As seen in the graph the lift coefficient of normal wing is more compared to the wing with groove. But the Drag Coefficient is less compared to the normal wing, this shows that the drag coefficient reduces when we build 7mm groove at 25% chord.

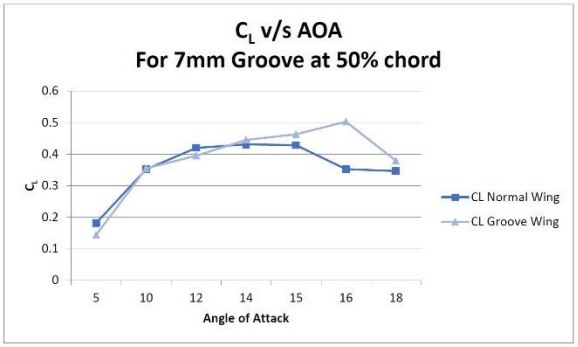

Fig 28: CL v/s AOA for Normal wing and 7mm groove at 50% chord wing

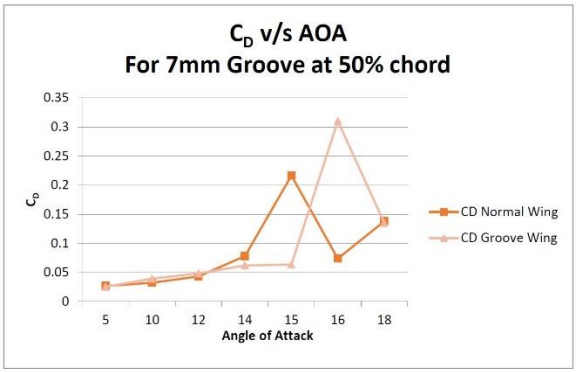

Fig 29: CD v/s AOA for Normal wing and 7mm groove at 50% chord wing

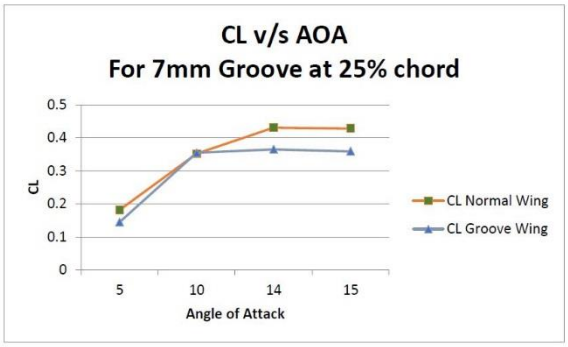

Fig 30: CL v/s AOA for Normal wing and 7mm groove at 25% chord wing

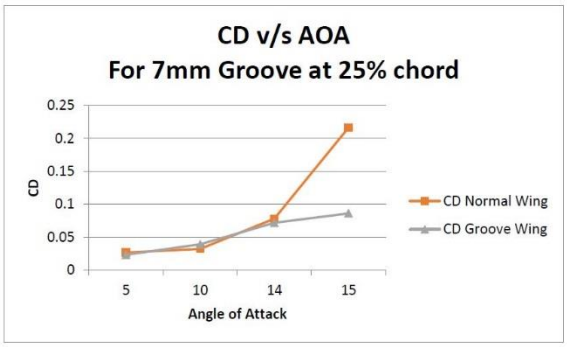

Fig 31: CD v/s AOA for Normal wing and 7mm groove at 25% chord wing

The comparison between the normal wing and 3mm groove wing at 10% chord is shown below in Fig 32 and Fig 33. As seen in the graph the lift coefficient of normal wing gradually decreases when the AOA increases and lift coefficient increases constantly. But the Drag Coefficient is customary compared to the normal wing as shown in the graph and there is a drastic change of drag coefficient of normal wing when there is rise in AOA as shown in the figure

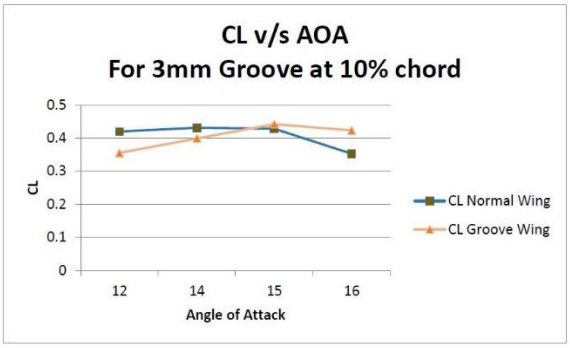

Fig 32: CL v/s AOA for Normal wing and 3mm groove at 10% chord wing

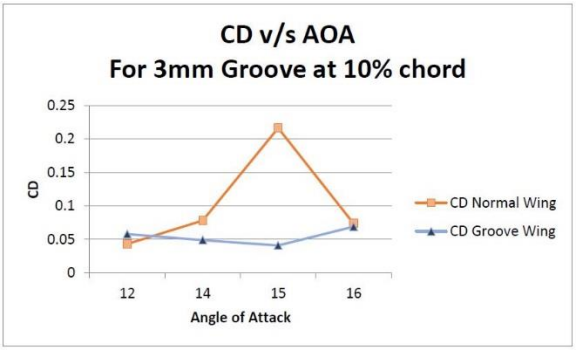

Fig 33: CD v/s AOA for Normal wing and 3mm groove at 10% chord wing

6. CONCLUSIONS

A study was done on the design and analysis of continuous groove effect on the wing for velocity 15m/s. For the experiment conducted for various groove sizes placed at different position and angle of attack. We come to know that groove placed at 50% of the chord with 7mm diameter gives the best lift to drag ratio by reattaching the flow, causing it to overcome the stall angle up to 16° when compared with the plain wing having a stall angle of 14.5°. The results for the computational study, we got improved values of CL= 0.5023 and CD= 0.3102 for the groove placed at 50% of chord with 7mm diameter whereas the plain wing has the CL= 0.431 and CD= 0.078 for same conditions. In this study, many continuous groove effect parameters have been addressed. it is a great challenge to simultaneously measure the data. Therefore, a verification experiment is favourable.

References

[1] Prasath M S & Irish Angelin (2017), "Effects of dimples on aircraft wing", vol 2 issue 5,

[2] Deepanshu Srivastav, "Flow control over air foil using different shaped dimples" IPCSIT vol.33. 2012

[3] Livya E, Anitha G, Valli P, "Aerodynamic Analysis of Dimple Effect on Aircraft Wing" International Journal of Mechanical, Aerospace, Industrial, Mechatronics and Manufacturing Engineering, Vol.9, No.2,2015.

[4] M. Moses Devaprasanna1& N. Maheswaran, "CFD study on aerodynamic effects of dimple on aircraft wings", IJESR, vol 6, issue 11.

[5] Chowdhury H, (2010) "A comparative study of golf ball aerodynamics".

[6] A Arun Kumar & T S Gowthaman (2017), "Numerical investigation over dimpled wings of an aircraft" IJRASET vol 5 issue 4.

[7] Mohanasaravanan P S "Flow analysis around the dimple wing on aircraft" International Journal of

Engineering Research Online, A peer Reviewed International Journal, Vol.3, No.2, 2015.

[8] Aerodynamics for Engineering Students (Seventh Edition), 2017

[9] John D. Anderson; "Fundamental of Aerodynamics", third edition.

[10] Lambert, S. and Morrison, J.F., "Fundamental Studies of Active Dimples", Aiaa-2006-3182, 2006

[11] Michael B. Patacsil., "Dimples On Wings", California Science Fair, 2010

[12] Chana R. and Vishwanathi, P. R., "Base Drag Reduction Caused By Riblets On A Gaw(2) Airfoil", National Aerospace Laboratories, Journal Of Aircraft, Volume 35. No. 6, November December 1998

[13] Reneaux, J., "Overview on Drag Reduction Technologies for Civil Transport Aircraft" European Congress on Computational Methods in Applied Sciences snd Engineering Eccomas, 2004.

[14] Zerihan, J., "An Investigation into the Aerodynamics of Wings in Ground Effect", Phd Thesis, University Southampton, School of Engineering, 2001.

[15] Mahon, S. and Zhang, X. "Computational Analysis of Pressure and Wake Characteristics on an Aerofoil in Ground Effect", Asme, 2005, 127, Pp 290-298